

22. W S Stiles, "A modified Helmholtz line element in brightness-colour space, *Proc. Phys. Soc. (London)*, 58 (1946) 41.
23. G Wyszecki and W S Stiles, "Color Science: Concepts and Methods, Qualitative Data and Formulae", (2nd edition), Jhon Wiley & Sons, 1982 .
24. A Yezzi, "Modified curvature motion for image smoothing and enhancement", *IEEE Trans. on Image Processing*, 7 (1998) 345-352 .

## References

1. L. Ambrosio and V. M. Tortorelli, "Approximation of functionals depending on jumps by elliptic functionals via  $\Gamma$ -convergence", *Comm. Pure Appl. Math.*, 43 (1990), 999-1036.
2. L. Ambrosio and V. M. Tortorelli, "On the approximation of free discontinuity problems", *Boll. Un. Mat. It.*, 7 (1992), 105-123.
3. E. Di Giorgi, M. Carriero, and A. Leaci, "Existence theorem for a minimum problem with free discontinuity set", *Arch. Rat. Mech. Anal.*, 108 (1989), 195-218.
4. L. M. J. Florac, A. H. Salden, B. M. ter Haar Romeny, J. J. Koenderink and M. A. Viergever, "Nonlinear Scale-Space", *Image and Vision Computing*, 13 (1995) 279-294.
5. H. Helmholtz von, "Handbuch der Psychologischen Optik", Voss, Hamburg, 1896.
6. R. Kimmel and R. Malladi and N. Sochen, "Images as Embedding Maps and Minimal Surfaces: Movies, Color, Texture, and Volumetric Medical Images", *Proc. of IEEE CVPR'97*, (1997) 350-355.
7. R. Kimmel and N. Sochen and R. Malladi, "On the geometry of texture", Report, Berkeley Labs. UC, LBNL-39640, UC-405, November, 1996.
8. R. Kimmel and N. Sochen and R. Malladi, "From High Energy Physics to Low Level Vision", *Lecture Notes In Computer Science: 1252*, First International Conference on Scale-Space Theory in Computer Vision, Springer-Verlag, 1997, 236-247.
9. R. Kimmel, "A natural norm for color processing", *Proc. of 3-rd Asian Conf. on Computer Vision*, Hong Kong, Springer-Verlag, LNCS 1351, 1998, 88-95.
10. E. Kreyszing, "Differential Geometry", Dover Publications, Inc., New York, 1991.
11. J. M. Morel and S. Solimini, Variational methods in image segmentation, Birkhauser, Boston, MA, 1995.
12. D. Mumford and J. Shah, "Optimal approximations by piecewise smooth functions and associated variational problems," *Comm. Pure Appl. Math.*, 42 (1989), 577-685.
13. A. M. Polyakov, "Quantum geometry of bosonic strings", *Physics Letters*, **103B** (1981) 207-210.
14. M. Proesmans and E. Pauwels and L. van Gool, "Coupled geometry-driven diffusion equations for low level vision", In Geometric-Driven Diffusion in Computer Vision, Ed. B. M. ter Haar Romeny, Kluwer Academic Publishers, 1994.
15. T. Richardson and S. Mitter, "Approximation, computation, and distortion in the variational formulation", In Geometric-Driven Diffusion in Computer Vision, Ed. B. M. ter Haar Romeny, Kluwer Academic Publishers, 1994.
16. Geometric-Driven Diffusion in Computer Vision, Ed. B. M. ter Haar Romeny, Kluwer Academic Publishers, 1994.
17. L. Rudin and S. Osher and E. Fatemi, "Nonlinear total variation based noise removal algorithms", *Physica D*, 60 (1991) 259-268.
18. N. Sochen and R. Kimmel and R. Malladi, "From high energy physics to low level vision", Report, LBNL, UC Berkeley, LBNL 39243, August, Presented in ONR workshop, UCLA, Sept. 5 1996.
19. N. Sochen and R. Kimmel and R. Malladi, "A general framework for low level vision", *IEEE Trans. on Image Processing*, 7, (1998) 310-318.
20. N. Sochen and Y. Y. Zeevi, "Images as manifolds embedded in a spatial-feature non-Euclidean space", November 1998, EE-Technion report no. 1181.
21. N. Sochen and Y. Y. Zeevi, "Representation of colored images by manifolds embedded in higher dimensional non-Euclidean space", IEEE ICIP'98, Chicago, 1998.

one dimensional curves as expected. The reason is our numerical approximation for  $E$ . We use an edge image with the same resolution as that of the original image, adding central difference approximation yield the edge regions. One possible solution is to apply the refined numerical approximation to the edge map as in [15]. Finally, in Figure 4 we apply the segmentation function  $E$  in the embedding space, to a noisy image. The source of the noise comes from a digital camera compression distortions, followed by a scanned version of a printout picture.



**Fig. 4.** The original noisy image is on the left, followed by the edge indicator field  $E$ , and the final result. Bottom line shows a zoom in on the original noisy on the left and filtered image.

## 6 Summary and Conclusions

We presented a generalization of the Mumford-Shah enhancement and segmentation method. The generalization is in two aspects: Multi-channel images, i.e. color images are analyzed, and the  $L_2$  measure is replaced by the Polyakov action. The generalization is a natural application of the Beltrami framework that represent images as an embedding map of the image manifold in a spatial-feature space.



**Fig. 3.** Upper row, left to right: The original image, followed by the final edge indicator function  $E$ , and the final image. At the bottom are zoom-in frames of a square section cropped from the initial and the final images.

## 5 Experimental results



**Fig. 2.** Upper row, left to right: The original noisy image, followed by the final edge indicator function  $E$ , and the final image. At the bottom are zoom-in frames of a square section cropped from the initial and final images.

We tested both cases, where the segmentation function  $E$  is defined on the image manifold and then on the embedding space. The time derivatives are approximated by an explicit forward numerical approximation (Euler scheme). The spatial derivatives were taken first by forward followed by backwards approximation, see [17]. This is a simple way to keep the numerical support tight and centralized. The examples demonstrate color image enhancement for both noisy and clean images. In all examples we set  $\alpha = 7 \cdot 10^{-2}$ ,  $\beta = 2 \cdot 10^{-4}$ ,  $c = 10^{-3}$ . We also decreased the value of  $c$  along the iterations by setting  $c^{n+1} = c^n / 1.002$ , as proposed in [15].

In Figure 2 we use the segmentation function  $E$  on the image flat manifold. The embedding space was taken Euclidean in color space. Figure 3 tests the segmentation function  $E$  on the embedding space. This example takes a clean benchmark image into a piecewise smooth one. Here the embedding space is based on Helmholtz's arclength in color  $ds_{color}^2 = (d \log R)^2 + (d \log G)^2 + (d \log B)^2$ , see also [5, 22, 23, 20]. In some cases the edges appear as 'edge regions' rather than

where  $i = [R, G, B]$ , and

$$\Delta_g(X) = \frac{1}{\sqrt{g}} \partial_\mu (\sqrt{g} g^{\mu\nu} \partial_\nu X),$$

is the Laplace-Beltrami operator on the image manifold. The factor 2 in the first term of the equation for  $E$  comes from the choice of the metric as the induced one given in Eq. (10). We find that

$$g^{\mu\nu} (\partial_\mu I^i) (\partial_\nu I^j) h_{ij}(\mathbf{X}) = g^{\mu\nu} g_{\mu\nu} = \text{Tr}(\text{Id}_{2 \times 2}) = 2. \quad (18)$$

The first term in the equation for  $I$  smoothes the function when  $E = 1$  and is ineffective around an edge when  $E$  approaches zero. The second term sharpens gradients and create shocks. The last term pushes  $I$  towards  $I_0$ .

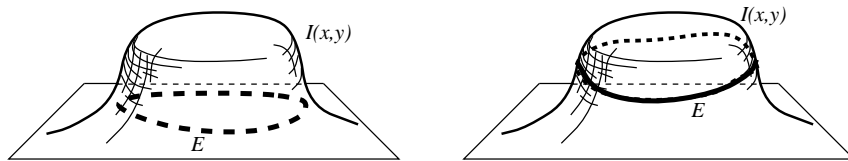


**Fig. 1.** Left is the edge indicator function  $E$  defined over the image plane  $\{x, y\}$ . Right: the edge indicator function  $E$  defined on the image surface manifold  $\{x, y, I(x, y)\}$ .

## 4.2 Segmenting function on the embedding space

The metric is, as before, the induced metric but this time the Polyakov action is used only for the feature coordinates. The segmenting function is defined over the Euclidean spatial part of the embedding space and therefor it is smoothed using the usual  $L_2$  norm. The functional, in this case, is

$$F_c[I^1, I^2, I^3, E] = \int_{\Sigma} d^2\sigma \sqrt{g} \left( \frac{\alpha}{2} (X^i - X_0^i) h_{ij}(\mathbf{X}) (X^j - X_0^j) + \frac{\beta}{2} E(x, y)^2 g^{\mu\nu} (\partial_\mu X^i) (\partial_\nu X^j) h_{ij}(\mathbf{X}) \right) + \int dx dy \left( \frac{c}{2} |\nabla E|^2 + \frac{(E-1)^2}{4c} \right) \quad (19)$$

The gradient descent equations are

$$I_t^i = \beta E^2 \Delta_g(I^i) + \beta g^{\mu\nu} (\partial_\mu E) (\partial_\nu I^i) - \alpha (I^i - I_0^i)$$

$$E_t = -2\beta \sqrt{g} E + \frac{1-E}{2c} + c \Delta(E),$$

where  $i=[R,G,B]$ , and  $\Delta(E)$  is the usual Laplacian. The first term in the equation for  $E$  decreases the values of  $E$  for large  $g$ . The second term of the equation pushes the values of  $E$  toward 1, as  $c$  approaches zero. The last term is a smoothing term.

spatial-color Riemannian manifold. The coordinates of the two-dimensional manifold are  $(\sigma^1, \sigma^2)$ , and those of the five-dimensional one are  $(X^1, X^2, X^3, X^4, X^5)$ . The embedding map is

$$\{X^1 = \sigma^1, X^2 = \sigma^2, X^3 = R(\sigma^1, \sigma^2), X^4 = G(\sigma^1, \sigma^2), X^5 = B(\sigma^1, \sigma^2)\}. \quad (15)$$

We identify  $X^1$  with  $x$  and  $X^2$  with  $y$  and by abuse of notations we write  $\{x, y, R(x, y), G(x, y), B(x, y)\}$ . We also use below the notation  $I^i$  for  $i = r, g, b$  to denote the different color channels.

The metric of the embedding space is

$$ds^2 = dx^2 + dy^2 + ds_{color}^2, \quad (16)$$

where the metric in the color space is model dependent, see [23] for a general discussion and [20, 21] for the analysis of different color models in the Beltrami framework. We choose, for sake of simplicity, to adopt a Euclidean metric for the color space, see [24] for a related effort.

Two different approaches are possible in the treatment of the segmenting function. We can think of it as a function on the image manifold or as a function on the spatial part of the embedding space. The two approaches lead to somewhat different equations even though the spatial part and the image manifold coordinates are identified in the embedding map.

#### 4.1 Segmenting function on the image manifold

The metric in the image manifold is given by the induced metric (see Eq. (10)). We assume further that the segmenting function is defined over the two-dimensional image manifold, see Figure 1. We use the Polyakov action as an adaptive smoothing metric for both the color coordinates and the segmenting function. The functional we propose reads

$$F_c[I^1, I^2, I^3, E] = \int_{\Sigma} d^2\sigma \sqrt{g} \left( \frac{\alpha}{2} (X^i - X_0^i) h_{ij}(\mathbf{X}) (X^j - X_0^j) + \frac{\beta}{2} E (\sigma^1, \sigma^2)^2 g^{\mu\nu} (\partial_\mu X^i) (\partial_\nu X^j) h_{ij}(\mathbf{X}) + \frac{c}{2} g^{\mu\nu} (\partial_\mu E) (\partial_\nu E) + \frac{(E-1)^2}{4c} \right) \quad (17)$$

We take the color metric to be the unit matrix  $h_{ij} = \delta_{ij}$  from now on. We minimize this functional by the gradient descent method. Formally, the equations are

$$I_t^i \equiv \frac{\partial I^i}{\partial t} = -\frac{1}{\sqrt{g}} \frac{\delta F}{\delta I^i}$$

$$E_t \equiv \frac{\partial E}{\partial t} = -\frac{\delta F}{\delta E}.$$

The functional variations yield the following explicit partial differential equations

$$I_t^i = \beta E^2 \Delta_g(I^i) + \beta g^{\mu\nu} (\partial_\mu E) (\partial_\nu I^i) - \alpha (I^i - I_0^i)$$

$$E_t = -\sqrt{g} \left( 2\beta E - \frac{1-E}{2c} - c \Delta_g(E) \right)$$

Using standard methods in variation calculus, the Euler-Lagrange (EL) equations with respect to the embedding are (see [18] for derivation)

$$-\frac{1}{2\sqrt{g}}h^{il}\frac{\delta F}{\delta X^l} = \Delta_g X^i + \Gamma_{jk}^i(\partial_\mu X^j)(\partial_\nu X^k)g^{\mu\nu}, \quad (11)$$

where the operator that is acting on  $X^i$  in the first term is the natural generalization of the Laplacian from flat spaces to manifolds and is called *the second order differential parameter of Beltrami* [10], or in short *Beltrami operator*. It is given in term of the metric as

$$\Delta_g X^i = \frac{1}{\sqrt{g}}\partial_\mu(\sqrt{g}g^{\mu\nu}\partial_\nu X^i). \quad (12)$$

In the second term of Eq. (11), the  $\Gamma_{jk}^i$  are the Levi-Civita connection's coefficients with respect to the metric  $h_{ij}$  that describes the geometry of the embedding space [23]

$$\Gamma_{jk}^i = \frac{1}{2}h^{il}(\partial_j h_{lk} + \partial_k h_{jl} - \partial_l h_{jk}). \quad (13)$$

This term is in particular important in color image analysis and processing since some of the models of color perception assume non-Euclidean color space.

We view scale-space as the gradient descent,

$$X_t^i \equiv \frac{\partial X^i}{\partial t} = -\frac{1}{2\sqrt{g}}h^{il}\frac{\delta F}{\delta X^l}. \quad (14)$$

Notice that we used our freedom to multiply the Euler-Lagrange equations by a strictly positive function and a positive definite matrix. This factor is the simplest one that does not change the minimization solution while giving a reparameterization invariant expression. This choice guarantees that the flow is geometric and does not depend on the parameterization.

Choosing the induced metric and minimizing the feature coordinates results in a system of coupled partial differential equations that describe the flow of the image surface inside the spatial-feature space. This flow has the effect of smoothing more rapidly areas between edges than the edges themselves. This effect is achieved by the projection of the mean curvature vector to the feature space. Since normals to the surface at an edge lie almost entirely in the spatial space, their projection to the feature space is small and does not change the value or location of an edge.

This technique was used to denoise and enhance a variety of gray-level, color, 3D images, like movies, and volumetric medical images, and texture [7, 19, 18]. Next, we show that it is a useful measure in color image segmentation.

## 4 Color Segmentation Functional

According to the Beltrami framework [19], a color image is represented as an embedding map of a two-dimensional Riemannian manifold in a five-dimensional



where  $a$ ,  $b$ ,  $c$  and  $f$  are functions of  $x$  and  $y$ , and  $f$  is positive definite. The interpretation of this generalization is geometric. Images are viewed as embedding maps. Let us consider the important example  $\mathbf{X} : \Sigma \rightarrow \mathbb{R}^3$ . Denote the local coordinates on the two-dimensional manifold  $\Sigma$  by  $(\sigma^1, \sigma^2)$ , these are analogous to arc-length for the one-dimensional manifold, i.e. a curve. The map  $\mathbf{X}$  is explicitly given by

$$(X^1(\sigma^1, \sigma^2) = \sigma^1, X^2(\sigma^1, \sigma^2) = \sigma^2, X^3(\sigma^1, \sigma^2) = I(\sigma^1, \sigma^2)). \quad (6)$$

Since the local coordinates  $\sigma^i$  are curvilinear, the squared distance is given by a positive definite symmetric bilinear form called the metric whose components are denoted by  $g_{\mu\nu}(\sigma^1, \sigma^2)$ ,

$$ds^2 = g_{\mu\nu} d\sigma^\mu d\sigma^\nu \equiv g_{11}(d\sigma^1)^2 + 2g_{12}d\sigma^1 d\sigma^2 + g_{22}(d\sigma^2)^2, \quad (7)$$

where we used Einstein summation convention in the second equality; identical indices that appear one up and one down are summed over, see [4, 18] for a short introduction to tensor calculus and covariance in the context of image analysis. We denote the inverse of the metric by  $(g^{\mu\nu})$ , and its determinant by  $g$ .

The Polyakov action is a generalization of  $L_2$ . It depends on *both* the image manifold and the embedding space. Denote by  $(\Sigma, (g_{\mu\nu}))$  the image manifold and its metric and by  $(M, (h_{ij}))$  the space-feature manifold and its metric. We choose  $\rho(|\mathbf{s}|) = \mathbf{s} \cdot \mathbf{s} \equiv s^i s^j h_{ij}$ , then the map  $\mathbf{X} : \Sigma \rightarrow M$  has the following weight [13]

$$F[X^i, g_{\mu\nu}, h_{ij}] = \int d^m \sigma \sqrt{g} g^{\mu\nu} (\partial_\mu X^i) (\partial_\nu X^j) h_{ij}(\mathbf{X}), \quad (8)$$

where  $m$  is the dimension of  $\Sigma$  and the range of indices is  $\mu, \nu = 1, \dots, \dim \Sigma$ , and  $i, j = 1, \dots, \dim M$ . In the above expression  $d^m \sigma \sqrt{g}$  is a volume element of the image manifold. The rest, i.e.  $g^{\mu\nu} (\partial_\mu X^i) (\partial_\nu X^j) h_{ij}(\mathbf{X})$ , is a generalization of  $L_2$ . It is important to note that this expression, as well as the volume element, do not depend on the local coordinates one chooses.

For our example in Eq. (6), we assume a diagonal form for the embedding space, i.e.  $h_{ij}(x, y, I) = f_i(x, y, I) \delta_{ij}$  (no summation over indices here). We get the following functional

$$F[I, g_{\mu\nu}] = \int dx dy \sqrt{g} (g^{11} f_1 + g^{22} f_2 + (g^{11} I_x^2 + 2g^{12} I_x I_y + g^{22} I_y^2) f_3) \quad (9)$$

which is reduced, up to terms independent of  $I$ , to the form of the functional in Eq. (5) when the  $f_i$ 's are constants.

The minimization of  $F$  with respect to the metric can be solved analytically, for two-dimensional manifolds. The minimizing metric is the induced metric of the isometric embedding. Explicitly, it is given in terms of the embedding map and the metric of the embedding space,

$$g_{\mu\nu}(\sigma^1, \sigma^2) = h_{ij}(\mathbf{X}) (\partial_\mu X^i) (\partial_\nu X^j). \quad (10)$$

total length of the discontinuity set. The implicit assumption that underlies this functional is that an image is a piecewise smooth function. The first term penalizes a function that differs from the observed one, the second term penalizes large gradients, and the last term penalizes excessive use of segmentation curves. The minimizer places the segmenting curves along the most significant gradients and tries to smooth the function everywhere else without diverting too much from the original image. The parameters  $\alpha$  and  $\beta$  control the relative weight of the three terms.

It is difficult to minimize this functional numerically because of the large number of possibilities of placing the set of boundaries  $K$  inside  $\Omega$ . In order to have a better control of the problem, both mathematically and numerically, it is convenient to approximate the functional. In the  $\Gamma$ -convergence framework, a new functional is proposed [2] in the form

$$F_c[I, E] = \int_{\Omega} (\alpha(I - I_0)^2 + \beta E^2 |\nabla I|^2 + c|\nabla E|^2 + \psi_c(E)) \, dx dy, \quad (2)$$

where, ideally the function  $E(x, y)$  is an edge indicator, such that  $E(x_0, y_0) = 0$  when an edge passes through  $(x_0, y_0)$  and  $E(x, y) = 1$  otherwise. In this case, the second term in the approximating functional is identical to the second term in the Mumford-Shah functional. In fact, we demand that the segmenting function  $E$  is a smooth function and use the  $L_2$  norm to penalize discontinuities in  $E$ . The last term is constructed in such a way that it forces  $E$  to behave as an edge indicator, i.e. it pushes  $E$  to 1 far from an edge. In the vicinity of an edge, the term  $E^2 |\nabla I|^2$  pushes  $E$  to zero. Explicitly, Ambrosio and Tortorelli have chosen:

$$F_c[I, E] = \int_{\Omega} \left( \alpha(I - I_0)^2 + \beta E^2 |\nabla I|^2 + c|\nabla E|^2 + \frac{(E - 1)^2}{4c} \right) \, dx dy. \quad (3)$$

One can show that in the limit as  $c \rightarrow 0$ , the functional  $F_c[I, E]$  approaches  $F[I, K]$  such that the minimizers of  $F_c$  converge to the minimizer of  $F$ .

One can naturally envisage using a different norm, i.e.  $L_1$  norm for the gradients of the denoised image and the segmenting function. The question is how to extend this idea for a color image.

### 3 The Polyakov action

Let us introduce a geometric viewpoint that enables us to generalize an adaptive smoothing algorithm to a higher dimensional and codimensional images.

There is an extensive literature on functionals of the type

$$F[I] = \int dx dy \rho(|\nabla I|) = \int dx dy \rho \left( \sqrt{I_x^2 + I_y^2} \right), \quad (4)$$

where  $\rho(s)$  is a function which has a lower bound. We suggest to generalize it in the following way:

$$F[I, a, b, c] = \int dx dy f(a, b, c) \rho \left( \sqrt{aI_x^2 + 2bI_x I_y + cI_y^2} \right), \quad (5)$$

around the edges. The degree of smoothness depends on the approximation parameter, and the function approaches a Dirac delta function for the edges, as the approximation parameter approaches zero.

In this study we address the question of the generalization of this approach to color images. Methods that disregard the coupling between the spectral channels give up important information given by the correlation between the color channels. Moreover, there is an underlying assumption in the Mumford-Shah model of the smoothness of the image in the non-boundary regions, which is formulated through an  $L_2$  measure. It is known, though, that the  $L_1$  performs better as an adaptive smoothing measure [17]. It is desirable, therefore, to incorporate the  $L_1$  norm or another adaptive smoothing scheme in the Mumford-Shah formulation for the segmentation problem. Recently, it was shown [19] that the Beltrami framework provides a proper generalization of the  $L_1$  norm from gray-level to color images.

In the Beltrami framework, an image is treated as a two-dimensional Riemannian surface, restricted as a graph, embedded in a higher dimensional spatial-feature space. A grey-level image is embedded in  $\mathbb{R}^3$  whose coordinates are  $(x, y, I)$  and it is simply the graph of the intensity function  $I(x, y)$ . Similarly, a color image is embedded in a five-dimensional space whose coordinates are  $(x, y, R, G, B)$ . The induced metric of these surfaces is easily extracted and a measure, known as the Polyakov action in high-energy physics, is used as a generalization of the  $L_2$  norm to any dimension and codimension, and for any geometry of the surface and of the embedding space. We and others have shown that this “geometric  $L_2$ ” norm interpolates via a scaling parameter between the conventional, i.e. flat  $L_1$  and  $L_2$  norms for gray level images. It interpolates, for color images, between the flat  $L_2$  and a different norm, which is interpreted as the proper generalization of the Euclidean  $L_1$  norm for color images [9, 6].

Our current study merges the  $\Gamma$ -convergence technique and the Beltrami framework for color images to yield a color and smoothing generalization for the Mumford-Shah segmentation functional.

The paper is organized as follows: In Section 2 we briefly review the  $\Gamma$ -convergence and its application for the gray-level image segmentation. Section 3 reviews the Beltrami framework. We present, in Section 4, our color segmentation functional and derive a non-linear coupled Partial Differential Equations (PDE) as gradient descent equations for this functional. Results are presented in Section 5, and we summaries and conclude in Section 6.

## 2 $\Gamma$ -Convergence Formulation

The Mumford-Shah functional includes three terms: A fidelity term, a smoothing term, and a penalty on the total length of the discontinuities. Let

$$F[I, K] = \int_{\Omega \setminus K} (\alpha(I - I_0)^2 + \beta|\nabla I|^2) dx dy + \mathcal{H}(K) \quad (1)$$

where  $I_0$  is the observed image,  $I$  is the denoised image,  $\Omega$  is the images domain, and  $K$  is the set of discontinuities. The Hausdorff measure  $\mathcal{H}(K)$ , measures the

# Geometric-Variational Approach for Color Image Enhancement and Segmentation

Ron Kimmel<sup>1</sup> and Nir A. Sochen<sup>2</sup>

<sup>1</sup> CS Department, Technion - Israel Institute of Technology  
Technion City, Haifa 32000, ISRAEL  
ron@cs.technion.ac.il,

WWW home page: <http://www.cs.technion.ac.il/~ron>

<sup>2</sup> EE Department, Technion - Israel Institute of Technology  
Technion City, Haifa 32000, ISRAEL  
sochen@ee.technion.ac.il

**Abstract.** *We merge techniques developed in the Beltrami framework to deal with multi-channel, i.e. color images, and the Mumford-Shah functional for segmentation. The result is a color image enhancement and segmentation algorithm. The generalization of the Mumford-Shah idea includes a higher dimension and codimension and a novel smoothing measure for the color components and for the segmenting function which is introduced via the  $\Gamma$ -convergence approach. We use the  $\Gamma$ -convergence technique to derive, through the gradient descent method, a system of coupled PDEs for the color coordinates and for the segmenting function.*

## 1 Introduction

Segmentation is one of the important tasks of image analysis and much efforts have been consecrated to solve it. One can roughly classify the segmentation methods into two classes: 1) Global, i.e. histogram based techniques, and 2) Local, i.e. edge based techniques. In the second class it was shown that a large number of algorithms, including different region growing methods coupled with edge detection based techniques, are closely related to the Mumford-Shah functional minimization [11]. This functional involves an interplay between an image, which is a two dimensional object, and the contours that surround the objects in the image, which are one-dimensional curves. This functional was first suggested and analyzed by Mumford and Shah for gray-level images in [12]. It was later extensively studied, see e.g. [11] for an overview.

In particular, the  $\Gamma$ -convergence framework [1–3, 15] was invented to overcome the problem of dealing with objects with different dimensionalities in the same functional. In the  $\Gamma$ -convergence framework, one replaces the functional by a different, parameter dependent, functional. The parameter controls the degree of approximation, such that the approximating functional is equal to the Mumford-Shah functional in the limit, as the parameter goes to zero. In the approximating functional, the edge contours are replaced by a two-dimensional function which is close in shape to an edge indicator with certain smoothness